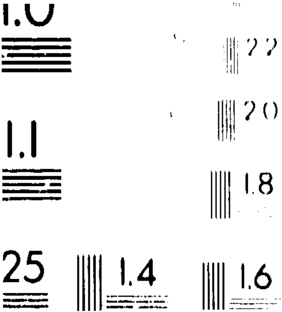
1.0
2.2
2.0
1.1
1.8
25
1.4
1.6

CONF- 891019--1

LA-UR--89-2930

DE89 016968

[illegible] for the United States Department of Energy under contract W-7405-ENG-36

TITLE: **FORMATION AND MODIFICATION OF SURFACE ALLOYS BY EXCIMER LASER MELTING AND RESOLIDIFICATION**

AUTHOR(S): Thomas R. Jervis, MST-7
Michael Nastasi, MST-7
Juha-Pekka Hirvonen, MST-7

SUBMITTED TO: Manuscript of invited paper to be presented at the Symposium on Microelectronic Integrated Processing and published in the Proceedings thereof.
Sponsored by the S.P.I.E.
October 8-13, 1989

DISCLAIMER

This report was prepared as an account of work sponsored by an agency of the United States Government. Neither the United States Government nor any agency thereof, nor any of their employees, makes any warranty, express or implied, or assumes any legal liability or responsibility for the accuracy, completeness, or usefulness of any information, apparatus, product, or process disclosed, or represents that its use would not infringe privately owned rights. Reference herein to any specific commercial product, process, or service by trade name, trademark, manufacturer, or otherwise does not necessarily constitute or imply its endorsement, recommendation, or favoring by the United States Government or any agency thereof. The views and opinions of authors expressed herein do not necessarily state or reflect those of the United States Government or any agency thereof.

Received by OSTI

By acceptance of this article, the publisher recognizes that the U.S. Government retains a nonexclusive, royalty-free license to publish or reproduce the published form of this contribution, or to allow others to do so, for U.S. Government purposes.

The Los Alamos National Laboratory requests that the publisher identify this article as work performed under the auspices of the U.S. Department of Energy.

MASTER

Los Alamos
Los Alamos National Laboratory
Los Alamos, New Mexico 87545

1190-18

Formation and modification of surface alloys by excimer laser melting and resolidification

T. R. Jervis, M. Nastasi, and J-P. Hirvonen

Materials Science and Technology Division
Los Alamos National Laboratory, Los Alamos, NM 87545

ABSTRACT

The use of pulsed lasers operating in the ultra-violet for the formation and modification of metal alloys opens a range of processing techniques which offer the precision of ion beam techniques but at much higher processing rates. In addition, excimer laser surface processing offers the possibility of new surface modification technologies. Most metals have low reflectivities in the UV, so laser light is coupled strongly to the surface. The short pulse length of these lasers, along with a shallow absorption depth, results in a heated zone which is also quite shallow, of the order of 1 micrometer. Modest fluences, of the order of 1 $J\text{-}cm^{-2}$ are sufficient to melt this surface zone. Typical quench rates from the melt are of the order of 10^{10} $K\text{-}sec^{-1}$; high enough to produce amorphous phases in some materials. Mixing by liquid phase diffusion between layers of vacuum evaporated materials and zone refinement can result from multiple melt resolidification events. These techniques make available a large range of alloy compositions on engineering materials. The surface morphology of the processed layers is quite smooth with a surface finish less than 100 nm. Further processing prior to use is therefore not required for most applications. We have studied laser mixing of metals into engineering materials, both metal alloys and ceramics, the formation of ceramic structures on metals, the modification of alloys by surface zone refinement, and the mixing of binary and ternary multilayer structures.

1. INTRODUCTION

The use of beam technologies to change the alloy composition and microstructure of the near surface region has been extensively studied in many materials[1-11]. The use of ion implantation, for example, is widespread in the semiconductor industry[12] and ion implanted materials are in use in tribological and corrosion applications[13]. The use of CO_2 lasers in industry is likewise widespread for cutting, joining, heat treating, and cladding applications[14]. Excimer lasers, however, are only beginning to make their presence known in industrial applications. Because of the short wavelengths available, the use of excimer lasers in photolithographic applications is growing, driven by the need for smaller device structures. This paper will discuss the use of ultra violet (UV) excimer lasers to melt, mix, and/or otherwise change the surface composition and microstructure of materials. The emphasis will be on metals and ceramics, but the same general lessons can be applied equally to semiconductor device applications.

One of the major benefits of ion implantation is its ability to place virtually any atomic species into any substrate in precise concentrations limited only by sputtering yields[15]. This is particularly useful in the semiconductor industry where selective doping is desired. However, the resulting surfaces are in a highly nonequilibrium condition. In semiconductors, this requires annealing to heal damage and activate the dopant. In other applications, it may mean that heat, work damage, or other stresses will cause the modified surface layer to transform to a condition closer to equilibrium. Thus end use applications require that the modified surface be in some equilibrium condition, even if that be a metastable equilibrium.

The differences between processing using CO_2 or Nd-YAG lasers and excimer lasers is summarized in Table 1. In the infrared (IR), most metals are good reflectors and many ceramics are transparent. In either case, coupling energy from the laser beam to the surface is a problem. The coupling process, and the use of various techniques to increase the efficiency of IR coupling has been extensively discussed elsewhere[ ] and will not be repeated here. In addition,because of the relatively long pulse length, melt depths are much larger, with concomitant changes in surface relief. The essential point is that much more incident laser energy is required to have the same thermal effect as with excimers and the result is a larger *scale* of effects. This can be an advantage in some applications (cutting and welding in particular) but processing with a scale depth or surface relief of 100's or even 10's of microns is not applicable to the semiconductor industry.

Laser	Excimer (KrF)	CO_2/Nd-YAG
Wavelength	0.248 µm	10.6/1.06 µm
Absorptivity	~ 50%	~ 0.1%
Melt Depth	~ 1 µm	~ 100 µm
Melt Duration	~ 100 nsec	~ 100 µsec
Cooling Rate	~ 10^{10} K/sec	~ 10^{6} k/sec
Processing Rate	~ 1 cm^2/sec	~ 1 cm^2/sec
Power Required	~ 10 W	~ 10 KW

Table 1. Comparison of material processing parameters for UV and IR lasers.

The use of excimer lasers for surface processing can overcome some of the problems inherent in both ion implantation or related ion mixing and IR laser technologies. The shallow melt depth and short pulse duration result in surface relief in melted metal systems of less than 0.1 µm. Because the processing is essentially thermal in nature, the system has a chance to come to an equilibrium point. Although the melt duration for a single pulse is short, liquid state diffusion can occur to lengths of the order of 5 nm and with multiple pulses mixing and/or segregation over substantial distances is possible. The very high solidification rate also often results in metastable equilibrium, a desirable feature in many systems. Ion implantation requires a substantial investment in capital equipment (the implanter) and must be done in vacuum. Lasers are relatively cheap and processing requires at most a shield gas, substantially reducing the complexity of the process. Finally, since excimer lasers are comparably efficient to CO_2 lasers in converting electrical to photon energy, substantial energy savings are available for those applications where excimers can replace IR lasers.

2. COUPLING AND THERMAL EFFECTS

Excimer laser radiation is absorbed within a very short distance in virtually all materials. Typical absorption depths in metals are of the order of 3 nm. Absorption, typically in electron shells, is rapidly thermalized to a heat pulse which is conducted away from the surface. Obviously, there is radiation from the hot surface and convection at the free surface, but these effects are relatively minor at the temperatures and times which of of concern here. The surface of the material melts and the melt front propagates inward until the energy of the pulse is dissipated in the melt process. The melt front then stops and a resolidification front moves back toward the surface. The time history of the temperature of the melted surface layer of metals can be calculated directly from the fundamental optical and thermal constants of the material. If we assume that the laser pulse has a square temporal profile, so that power incident is either a constant P_0 or zero, the temperature, T, of the material at any depth z and time t is given by[16, 17]:

$$T(z,t) = (1 - R)\,\frac{2P_0\sqrt{\kappa t}}{K}\,\mathrm{ierfc}\left(\frac{z}{2\sqrt{\kappa t}}\right) \quad \text{for } t \le t_0$$

and

$$T(z,t) = (1 - R)\,\frac{2P_0\sqrt{\kappa}}{K}\left(\sqrt{t}\;\mathrm{ierfc}\left(\frac{z}{2\sqrt{\kappa t}}\right) - \sqrt{t - t_0}\;\mathrm{ierfc}\left(\frac{z}{2\sqrt{\kappa(t - t_0)}}\right)\right)$$

for $t > t_0$

where:

R = reflectivity

κ = thermal diffusivity

K = thermal conductivity

t_0 = pulse length

Although this calculation ignores many significant aspects of the melt solidification process, such as the temperature dependence of many of the variables, it is useful in comparing the effects of laser light on different materials and is in fact not a bad predictor of what actually happens to materials under pulsed UV radiation. Table 2 gives laser melting parameters as calculated using this model, with the further assumption that melting occurs when the heat of fusion of the material is absorbed.

It is clear that cooling rate and melt duration are relatively insensitive to material parameters. The principal differences between materials being in melt depth and fluence required to melt. In all cases, the high cooling rates result in the material returning to the initial temperature within 0.01 to 0.1 sec, so that if repetition rates of less than 10 Hz are used, the effect of each pulse is independent. Obviously, if multiple pulses are used, total melt duration increases linearly with the number. Also, if fluences greater than this threshold value are used, greater melt depth and duration are possible, although the use of high fluences can be limited by ablation processes[18].

Material	Melt Fluence	Melt Depth	Melt Duration	Cooling Rate
304 SS	0.8 J/cm^2	0.25 μm	20 nsec.	2 x 10^{10} K/sec
Ag	0.8 J/cm^2	0.95 μm	10 nsec.	2 x 10^{10} K/sec
Mo	4.0 J/cm^2	0.40 μm	15 nsec.	5 x 10^{10} K/sec
Be	1.2 J/cm^2	0.60 μm	20 nsec.	2 x 10^{10} K/sec
SiC	1.1 J/cm^2	0.29 μm	15 nsec.	4 x 10^{10} K/sec
ZrO	0.4 J/cm^2	0.15 μm	50 nsec.	1.5 x 10^{10} K/sec

Table 2. Excimer laser melting parameters for various materials. All values refer to values just above the melt threshold.

3. LASER SURFACE PROCESSING

Repeated melting and resolidification of the surfaces of metals can have interesting effects if appropriate driving forces exist. In the case of AISI 304 stainless steel, there is apparently a strong driving force for the formation of a Cr rich oxide on the surface. After multiple pulse laser processing, we find that the Cr content of the surface oxide is increased dramatically. Figure 1 shows the Cr concentration in the near surface region of multiple pulse processed 304 stainless steel. The data is from Auger electron spectroscopy and is normalized to the Fe content. The increase in the Cr concentration is a direct result of the number of pulses used[19]. An effect similar to zone refining occurs as the resolidification front sweeps Cr to the surface. Whether this result is in fact due to zone refinement of a greater than solid solubility concentration of Cr from the bulk of the material or to a driving force originating in the stability of the Cr oxide is not clear. In Figure 2 the oxygen signal from the Auger analysis is demonstrates that the thickness of the surface oxide is unchanged, even though this processing was done in air. This increase in the Cr content of the surface oxide has interesting implications for the corrosion properties of laser treated materials[20,21].

4. EXCIMER LASER MIXING

In Figure 3. we show the Rutherford Backscattering (RBS) spectrum showing the excimer laser mixing of a single 50 nm layer of Ti on AISI 304 stainless steel. The thermal properties of the stainless steel and the Ti are very similar so that in this case there is little thermal impedance mismatch between the surface layer and the substrate. In the as deposited film there is no Fe on the surface and the Ti peak, superimposed on the Fe, etc in the substrate is well delineated. After processing with 1, 2, and 4 pulses of excimer radiation at 1.3 J/cm^2, the Ti peak broadens, reflecting both the diffusion of Ti into the substrate and the diffusion of Fe into the surface layer. The broadening, as well as the amount of Fe at the surface, increases with the number of pulses, representing increased mixing. After 4 pulses, the microstructure of the surface film was found to be amorphous[22].

It is also possible to mix metals into ceramic substrates. Figure 4 shows the RBS spectrum of a single 100 nm layer of Ti on polycrystalline SiC. In this case the Ti peak is well separated from the Si substrate edge and the effect of the mixing on the Ti layer and the substrate is quite clear. The Ti layer broadens , reflecting diffusion processes augmented in this case by driving forces from the stability of the compounds produced, and Si appears in the surface layer. Reconstruction of the spectrum in the 10 pulse case is consistent with a 150 nm thick mixed surface layer of composition $Ti_{45}C_{37}Si_{17}W_{0.1}$. The W is a binder in the SiC. Analysis of the surface layer by X-ray diffraction shows the presence of the expected carbides and silicides[23]. Similar results have been found in the mixing of Ni on SiC and to some extent on Si_3N_4[24].

The results of laser mixing of a 100 nm layer of Si on Nb are shown in Figure 5. In each case shown here, 5 pulses were used but at different fluences. As in the previous examples, Nb diffuses into the Si surface layer and the Si peak, here superimposed on the Nb signal broadens as the Si diffuses into the substrate. Reconstruction of this spectrum indicates that a 200 nm thick surface layer of $NbSi_2$ with a graded interface is formed after 5 pulses at 1.7 J/cm^2. The mixing of Si on Nb is particularly interesting because attempts to mix this structure with ion beams were not successful. Apparently there is a kinetic barrier to ion beam mixing which is not effective in the laser mixing case becaause of the higher temperatures involved.

Figure 6 shows the results of laser mixing on a Fe-Ti-C multilayer structure. The as-deposited structure consisted of eleven alternating layers; four of Fe, four of Ti, and three of C deposited by the sequential electron beam evaporation of each component on a stainless steel substrate. The total thickness of the multilayer structure was The RBS spectrum shows the clearly modulated signal expected in the multilayer structure. After laser mixing with a single pulse at 1.1 J/cm^2, the modulated signal has largely disappeared, indicating that the multilayer structure is quite throughly mixed. After 10 pulses at the same fluence, not only has the modulated signal disappeared, but the Fe content of the surface layer has increased substantially. Because there is an effectively infinite supply of Fe in the substrate, there is a strong driving force for out -diffusion of Fe from the substrate. This multilayer structure is another example of a system which was resistant to ion mixing but which laser mixes readily[25].

5. DISCUSSION

In the examples discussed above, diffusion of constituents occurred in each case, but mixing or segregation occurred depending on the direction of the thermodynamic driving force involved. In the case of Si/Nb. we demonstrated that even when there are kinetic barriers to reactions induced by ion mixing or equivalently implantation, excimer laser mixing may be able to overcome these barriers. Conversely, it should be understood that compositions far from equilibrium will generally not be produced by laser mixing, although metastable phases such as amorphous metals may be. The use of excimer lasers in mixing or segregation experiments such as these is straightforward. An understanding of the processes involved may lead to further exploitation of the potential of this technique.

6. ACKNOWLEDGEMENTS

We would like to thank P Stupik and the personnel of the Los Alamos Ion Beam Materials Laboratory for assistance in this work. This work was supported by the U. S.

Department of Energy under contract No. W-7405-ENG-36 through the Los Alamos Center for Materials Science.

7. REFERENCES

1. **Laser and Electron Beam Solid Interactions and Materials Processing**, J. F. Gibbons, L. D. Hess, & T. W. Sigmon, Eds. Mat. Res. Soc. Symp. Proc. **1**, North Holland, Amsterdam, 1981.
2. **Laser and Electron Beam Interactions with Solids,** B. R. Appleton & G. K. Keller, Eds. Mat. Res. Soc. Symp. Proc. **4**, North Holland, Amsterdam, 1982.
3. **Laser Solid Interactions and Transient Thermal Processing of Materials**, J. Narayan, W. L. Brown, & R. A. Lemons, Eds. Mat. Res. Soc. Symp. Proc. **13**, North Holland, Amsterdam, 1983.
4. **Energy Beam-Solid Interactions and Transient Thermal Processing**, J. C. C. Fan & N. M. Johnson, Eds. Mat. Res. Soc. Symp. Proc. **23**, North Holland, Amsterdam, 1984.
5. **Ion Implantation and Ion Beam Processing of Materials**, G. K. Hubler, O. W. Holland, C. R. Clayton, & C. W. White, Eds. Mat. Res. Soc. Symp. Proc. **27**, North Holland, Amsterdam, 1984.
6. **Energy Beam-Solid Interactions and Transient Thermal Processing,** D. K. Biegelsen, G. A. Rozgonyi, & C. V. Shank, Eds. Mat. Res. Soc. Symp. Proc. **35**, Materials Research Society, Pittsburgh, PA, 1985.
7. **Beam-Solid Interactions and Phase Transformations**, H. Kurz, G. L. Olson, & J. M. Poate, Eds. Mat. Res. Soc. Symp. Proc. **51**, Materials Research Society, Pittsburgh, PA, 1986.
8. **Beam-Solid Interactions and Transient Processes**, M. O. Thompson S. T. Picraux, & J. S. Williams, Eds. Mat. Res. Soc. Symp. Proc. **74**, Materials Research Society, Pittsburgh, PA, 1987.
9. **Fundamentals of Beam-Solid Interactions and Transient Thermal Processing,** M. J. Aziz, L. E. Rehn, & B. Stritzker, Eds. Mat. Res. Soc. Symp. Proc. **100**, Materials Research Society, Pittsburgh, PA, 1988.
10. **Processing and Characterization of Materials Using Ion Beams**, L. E. Rehn, J. Greene, & F. A. Smidt, Eds. Mat. Res. Soc. Symp. Proc. **128**, Materials Research Society, Pittsburgh, PA, 1989.
11. **Rapid Thermal Processing of Electronic Materials**, S. R. Wilson, R. A. Powell, & D. E. Davies, Eds. Mat. Res. Soc. Symp. Proc. **92**, Materials Research Society, Pittsburgh, PA, 1987.
12. **Ion Beam Processes in Advanced Electronic Materials and Device Technology**, B. R. Appleton, F. H. Eisen, & T. W. Sigmon, Eds. Mat. Res. Soc. Symp. Proc. **45**, Materials Research Society, Pittsburgh, PA, 1985.
13. J. K. Hirvonen, *Ion Implantation in Tribology and Corrosion Science*, J. Vac. Sci. Technol. **15** 1662-1668 (1978).
14. **Laser Surface Treatment of Metals**, C. W. Draper & P. Mazzoldi, Eds. Martinus Nijhoff, Dordrecht, 1986.
15. **Ion Beam Modification of Materials**, B. M. Ullrich, Ed. North Holland, Amsterdam, 1985.
16. **Conduction of Heat in Solids,** H. S. Carslaw and J. C. Jaeger, Oxford Univ. Press, Oxford, 1959.
17. V. G. Gregson, *Laser Heat Treatment*, in **Laser Materials Processing**, M. Bass, Ed. North Holland, Amsterdam, 201-234, 1983.

18. F. Spaepen,*Themodynamics and Kinetics of Metallic Alloy Formation by Picosecond Pulsed Laser Irradiation*, in **Laser Surface Treatment of Metals**, C. W. Draper & P. Mazzoldi, Eds. Martinus Nijhoff, Dordrecht, 1986.
19. D. R. Baer, D. J. Frydrych, and T. R. Jervis, Near-Surface Chemistry and Corrosion Behavior of Excimer Laser Surface-Melted AISI Type 304 Stainless Steel, in **Environmental Degradation of Ion and Laser Beam Treated Surfaces,** G. S. Was & K. Grabowski, Eds. The Metallurgical Society, Warrendale, PA 1989
20. T. R. Jervis, D. J. Frydrych, & D. R. Baer, *Effect of Excimer Laser Melting on the Near Surface Chemistry and Corrosion Properties of AISI 304 Stainless Steel*, Materials Letters **6** 225-226 1988.
21. T. R. Anthony & H. E. Cline, *Surface Normalization of Sensitized Stainless Steel by Laser Surface Melting*, J. Appl. Phys. **49** 1248-1255 1978.
22. T. R. Jervis, M. Nastasi, T. G. Zocco, & J. A. Martin, *Formation of Amorphous Ti Alloy Layers by Excimer Laser Mixing of Ti on AISI 304 Stainless Steel*, Appl. Phys. Lett. **53** 75-77 1988.
23. T. R. Jervis, J-P. Hirvonen, M. Nastasi, & M. Cohen, *Laser Mixing of Ti on SiC*, in **Beam-Solid Interactions: Physical Phenomena**, P. Borgesen, J A. Knapp, & R. A. Zuhr, Eds. Mat. Res. Soc. Symp. Proc. in press, Materials Research Society, Pittsburgh, PA, 1990.
24. R. K. Singh, K. Jagannadham, & J. Narayan, Laser Surface Modifiction of Metal-coated Ceramics, J/ Mater. Res. 3 1119-1126 1988.
25. J-P. Hirvonen, M. Nastasi, & J. W. Mayer, *Microstructure of Ion-bombardedFe-Ti and Fe-Ti-C Multilayered Films*, J. Appl. Phys. **60** 980-984 1986.

FIGURE CAPTIONS

Figure 1. Chromium concentration (normalized to Fe) of the near surface region of AISI 304 stainless steel treated with excimer laser radiation. Cr enhancement is a function primarily of the number of melt resolidification cycles rather than the total energy deposited.

Figure 2. Oxygen concentration profile of the samples shown in Figure 1. The thickness of the oxide does not increase significantly, demonstrating that the principal effect of excimer laser processing is to enrich the oxide in Cr.

Figure 3. Rutherford backscattering spectrum showing laser mixing of 50 nm layer of Ti on AISI 304 stainless steel. Fe moves to the surface and the Ti peak broadens as Ti diffuses into the substrate.

Figure 4. Rutherford backscattering spectrum showing laser mixing of 100 nm layer of Ti on a SiC substrate. Si as well as a W binder moves to the surface and the Ti peak broadens as Ti diffuses into the substrate. X-ray diffraction indicates the presence of numerous carbides and silicides.

Figure 5. Rutherford backscattering spectrum showing laser mixing of 100 nm layer of Si on a Nb substrate. Reconstruction of this spectrum is consistent with a 200 nm layer of $NbSi_2$ with a graded interface to the Nb.

Figure 6. Rutherford backscattering spectrum showing laser mixing of 100 nm thick multilayer Fe-Ti-C structure on AISI 304 stainless steel. The "finger" structure is due to the multiple layers of the as deposited structure.

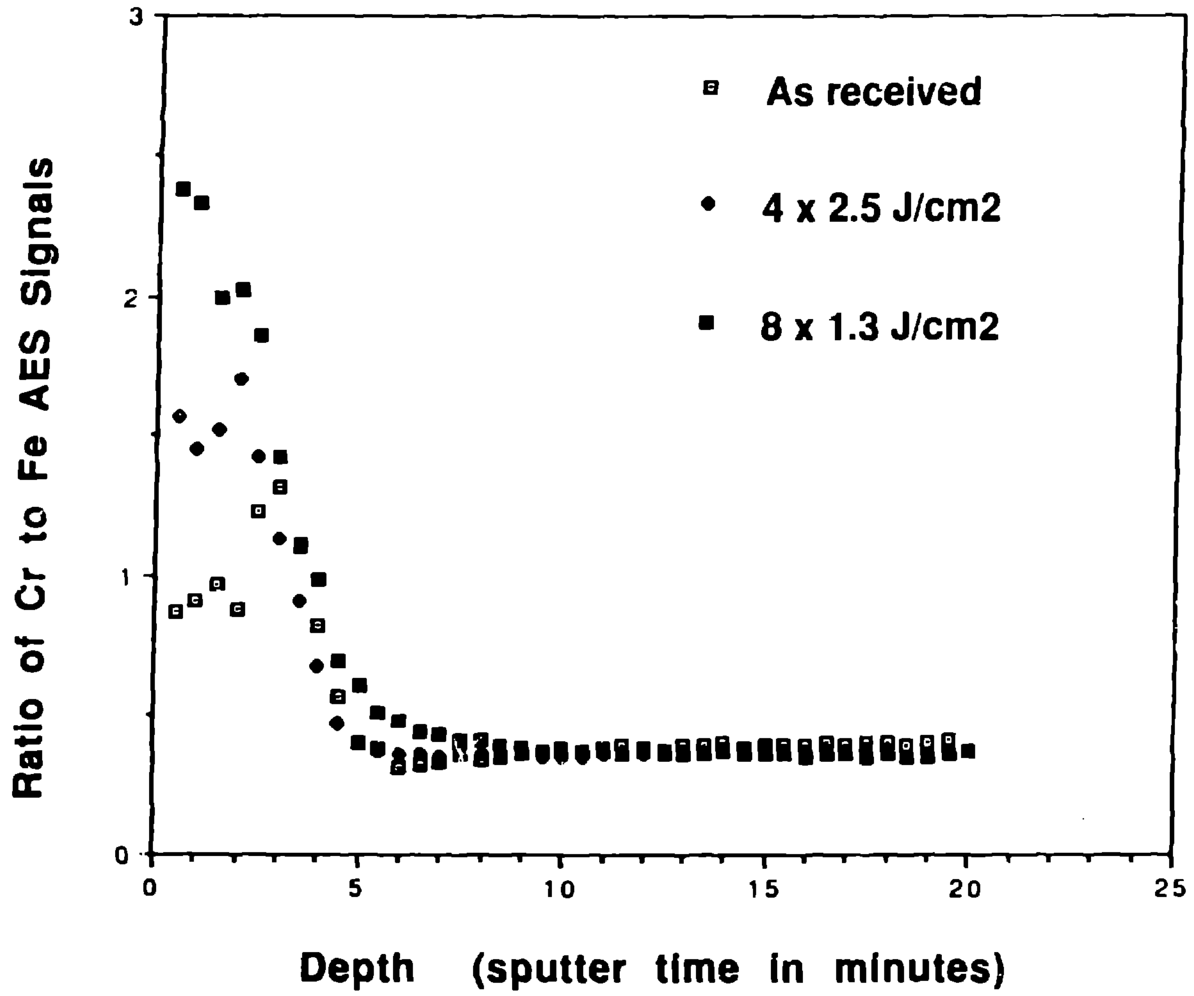
3
2
1
0
0
5
10
15
20
25
Ratio of Cr to Fe AES Signals
Depth (sputter time in minutes)
▫ As received
◆ 4 x 2.5 J/cm2
■ 8 x 1.3 J/cm2

Fig 1

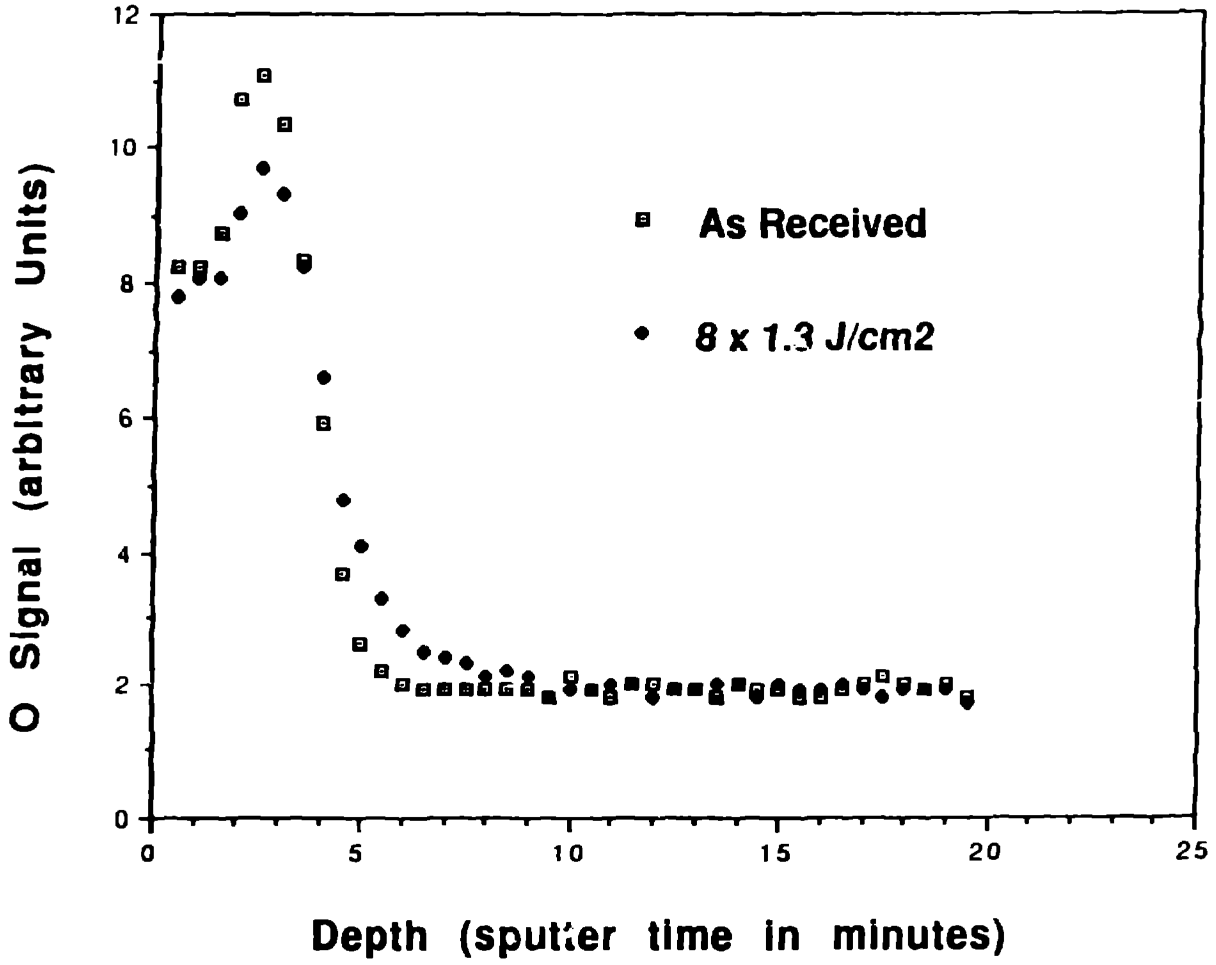
12
10
8
6
4
2
0
O Signal (arbitrary Units)
0
5
10
15
20
25
Depth (sputter time in minutes)
As Received
8 x 1.3 J/cm2

Fig. 2

Fig 3

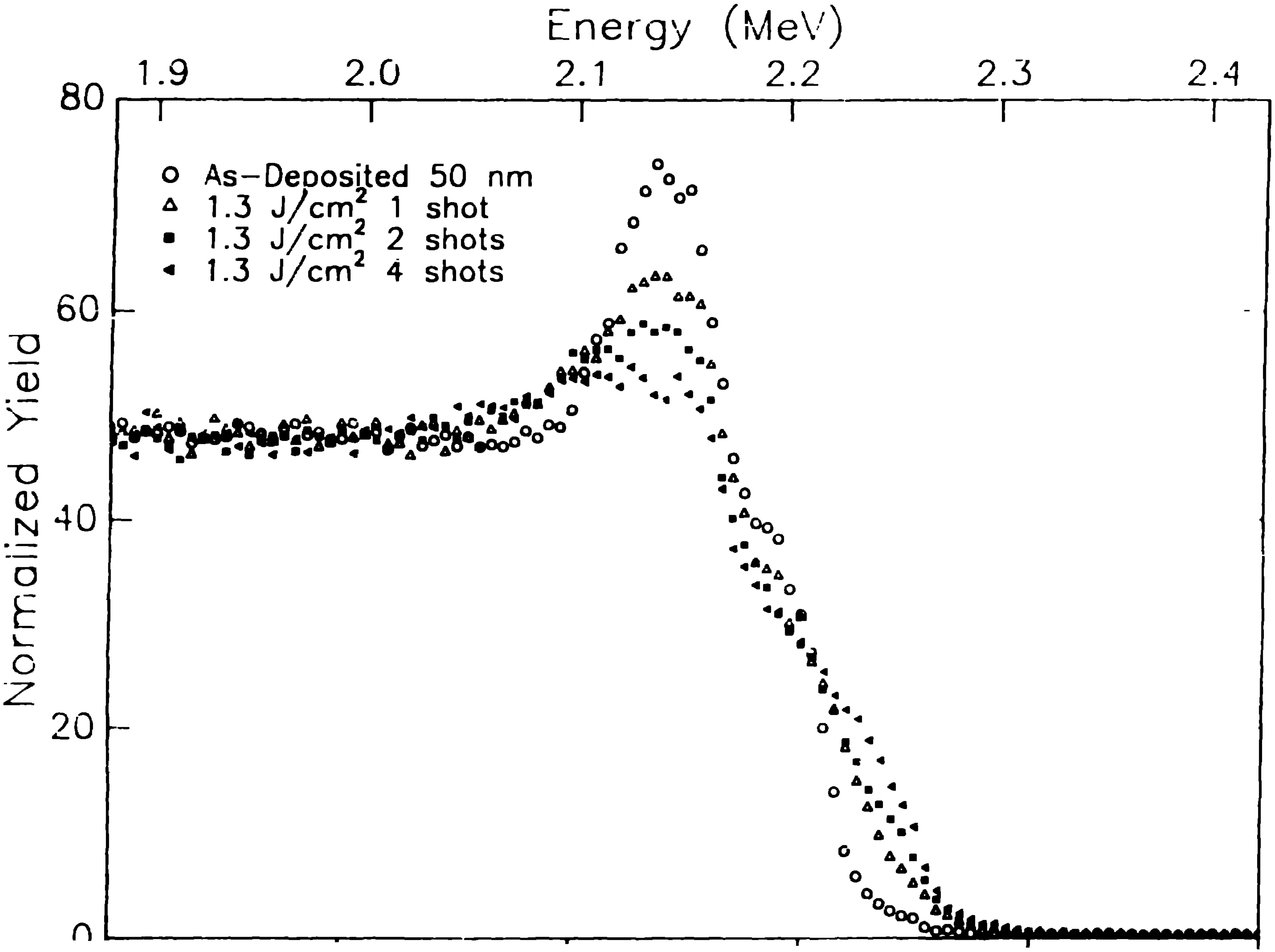
Energy (MeV)
1.9
2.0
2.1
2.2
2.3
2.4
80
60
40
20
0
Normalized Yield
○ As-Deposited 50 nm
△ 1.3 J/cm² 1 shot
■ 1.3 J/cm² 2 shots
◀ 1.3 J/cm² 4 shots

Fig 4

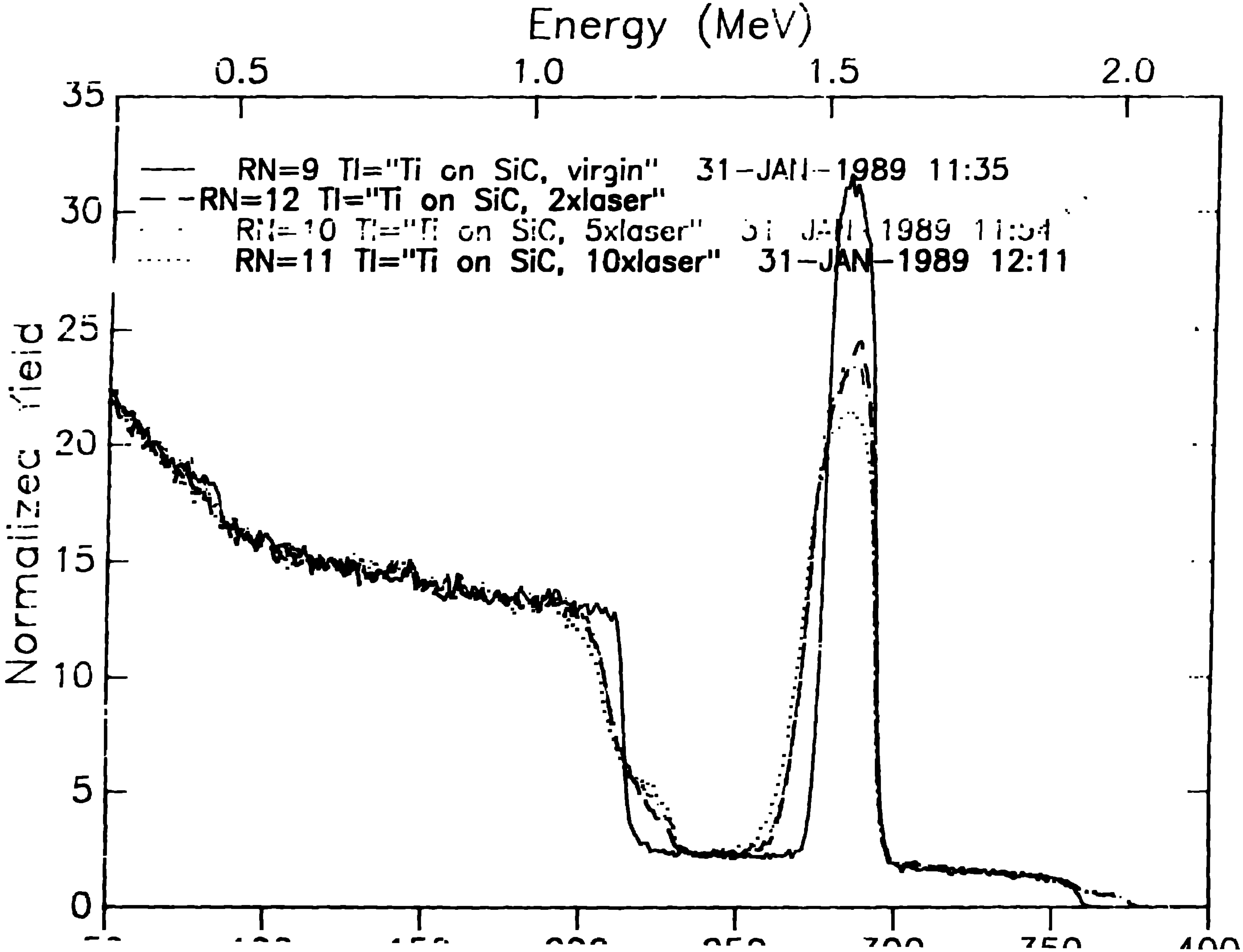
Energy (MeV)
0.5
1.0
1.5
2.0
35
30
25
20
15
10
5
0
Normalized Yield
RN=9 TI="Ti on SiC, virgin" 31-JAN-1989 11:35
RN=12 TI="Ti on SiC, 2xlaser"
RN=10 TI="Ti on SiC, 5xlaser" 31-JAN-1989 11:54
RN=11 TI="Ti on SiC, 10xlaser" 31-JAN-1989 12:11
400

Fig 5

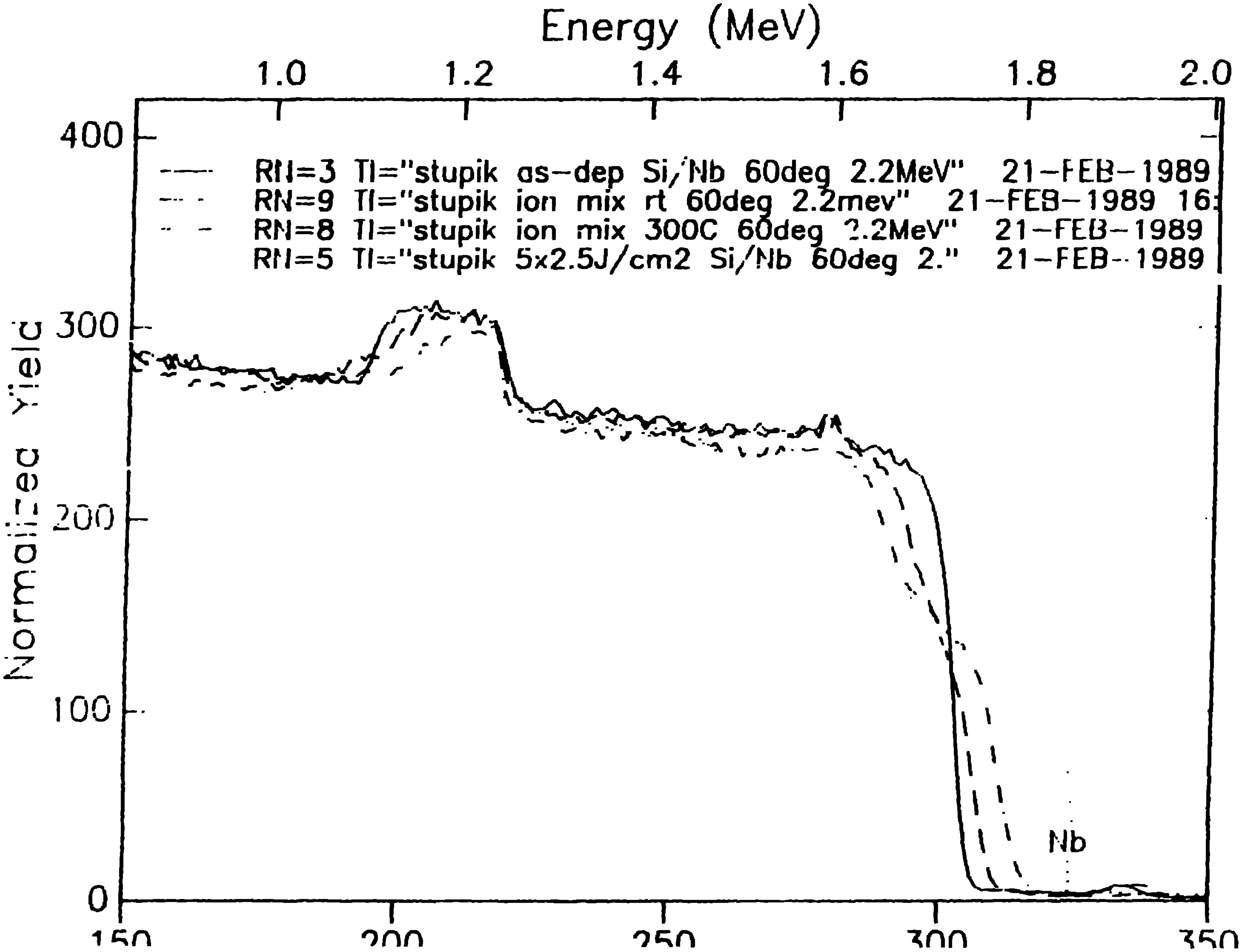
Energy (MeV)
1.0
1.2
1.4
1.6
1.8
2.0
400
300
200
100
0
Normalized Yield
RN=3 TI="stupik as-dep Si/Nb 60deg 2.2MeV" 21-FEB-1989
RN=9 TI="stupik ion mix rt 60deg 2.2mev" 21-FEB-1989 16:
RN=8 TI="stupik ion mix 300C 60deg 2.2MeV" 21-FEB-1989
RN=5 TI="stupik 5x2.5J/cm2 Si/Nb 60deg 2." 21-FEB-1989
Nb
150
200
250
300
350

Fig 6

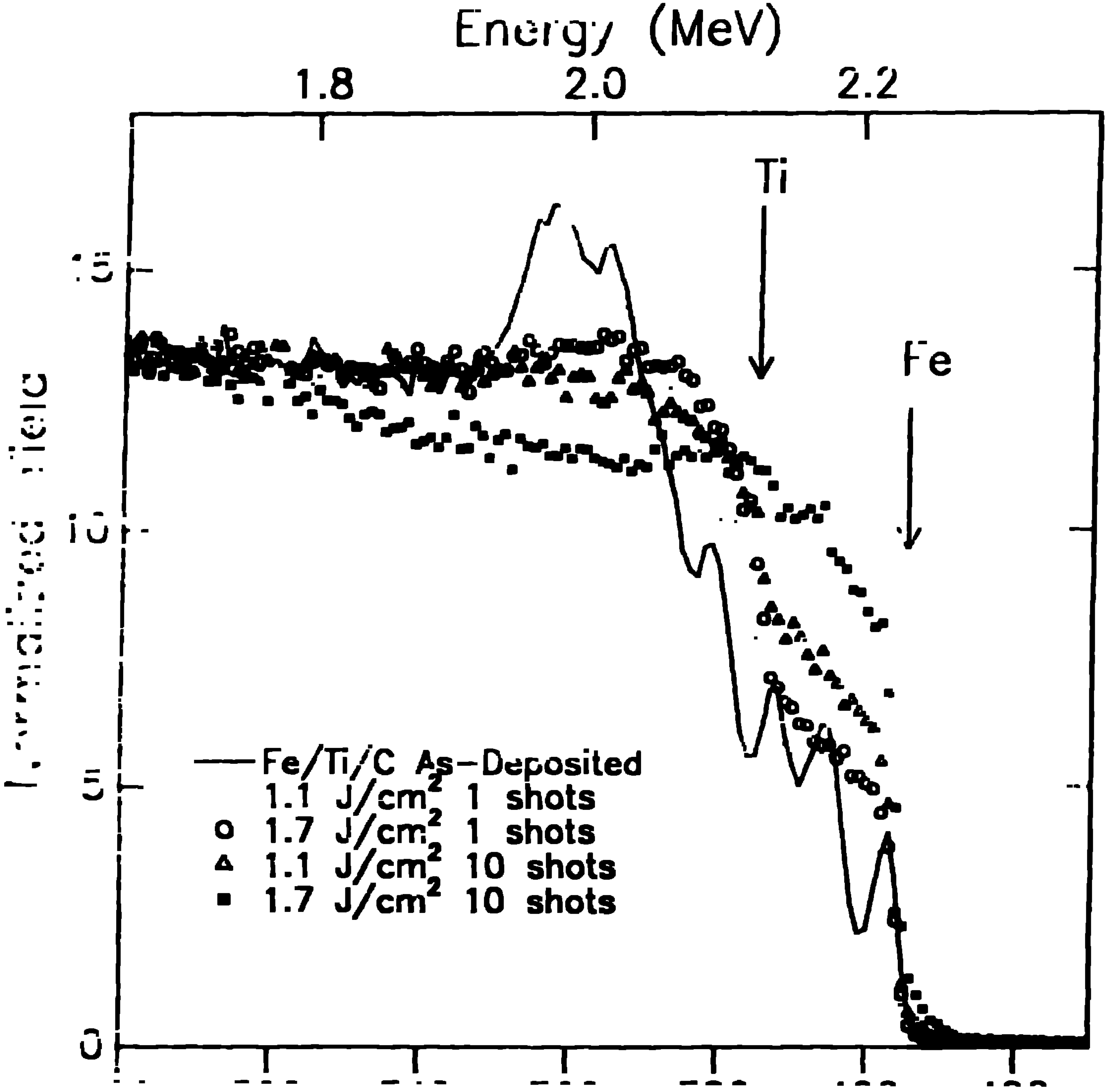
Energy (MeV)
1.8
2.0
2.2
Ti
Fe
Normalized Yield
15
10
5
0
Fe/Ti/C As-Deposited
1.1 J/cm2 1 shots
o 1.7 J/cm2 1 shots
△ 1.1 J/cm2 10 shots
■ 1.7 J/cm2 10 shots